Luteolin attenuates sepsis-induced myocardial injury by enhancing autophagy in mice

BIN WU[1*], HAIXU SONG[1*], MIAOMIAO FAN[1*], FEI YOU[2], LIANG ZHANG[1], JIAN LUO[3], JUNZHI LI[4], LINGPENG WANG[5], CONGYE LI[1] and MING YUAN[1]

[1]Department of Cardiology, Xijing Hospital, Fourth Military Medical University, Xi'an, Shaanxi 710032; [2]Department of Cardiology, Xi'an Central Hospital, Xi'an, Shaanxi 710004; Departments of [3]Internal Medicine (VIP), [4]Pathology and [5]Cardiology, First Affiliated Hospital, Xinjiang Medical University, Urumqi, Xinjiang 830000, P.R. China

Received June 26, 2019; Accepted January 28, 2020

DOI: 10.3892/ijmm.2020.4536

Abstract. Sepsis-induced cardiomyopathy (SIC) is a complication of severe sepsis and septic shock characterized by an invertible myocardial depression. This study sought to explore the potential effects and mechanism of luteolin, a flavonoid polyphenolic compound, in lipopolysaccharide (LPS)-induced myocardial injury. Experimental mice were randomly allocated into 3 groups (25 mice in each group): The control group (NC), the LPS group (LPS) and the LPS + luteolin group (LPS + Lut). Before the SIC model was induced, luteolin was dissolved in DMSO and injected intraperitoneally for 10 days into LPS + Lut group mice. NC group and LPS group mice received an equal volume of DMSO for 10 days. On day 11, the animal model of sepsis-induced cardiac dysfunction was induced by intraperitoneal injection of LPS. A total of 12 h after LPS injection, measurements and comparisons were made among the groups. Luteolin administration improved cardiac function, attenuated the inflammatory response, alleviated mitochondrial injury, decreased oxidative stress, inhibited cardiac apoptosis and enhanced autophagy. In addition, luteolin significantly decreased the phosphorylation of AMP-activated protein kinase (AMPK) in septic heart tissue. The protective effect of luteolin was abolished by 3-methyladenine (an autophagy inhibitor) and dorsomorphin (compound C, an AMPK inhibitor), as evidenced by decreased autophagic activity, destabilized mitochondrial membrane potential and increased apoptosis in LPS-treated cardiomyocytes, but was mimicked by 5-aminoimidazole-4-carboxamide ribonucleotide (an AMPK activator), suggesting that luteolin attenuates LPS-induced myocardial injury by increasing autophagy through AMPK activation. Luteolin may be a promising therapeutic agent for treating SIC.

Correspondence to: Professor Ming Yuan, Department of Cardiology, Xijing Hospital, Fourth Military Medical University, 127 Changle West Street, Xi'an, Shaanxi 710032, P.R. China
E-mail: yuanming@fmmu.edu.cn

*Contributed equally

Key words: sepsis-induced cardiomyopathy, luteolin, AMP-activated protein kinase, autophagy, lipopolysaccharide

Introduction

Sepsis is a condition that is often caused by a dysregulated host response to infection and can lead to life-threatening organ dysfunction (1). Despite abundant investigative attention towards advances in intensive care and supportive technology, sepsis remains in the top 10 leading causes of death and is a substantial cause of death among critically ill patients in non-coronary intensive care units (2,3). Sepsis is estimated to affect at least 19 million patients worldwide, reminding scientists and clinicians that it remains a serious global health burden and a major clinical challenge (4-6). Sepsis-induced cardiomyopathy (SIC) is a common complication of sepsis involving a combination of dysregulated inflammatory response, oxidative stress, calcium regulation disorder, dysregulated autonomic nervous system, impaired autophagy, apoptotic damage, mitochondrial dysfunction and endothelial dysfunction (7-9). Despite more aggressive approaches to prevent the progression of SIC, these strategies often turn out to be disappointing and the mechanisms of SIC are currently poorly elucidated.

Luteolin, a common bioactive flavonoid polyphenolic compound, can be isolated from numerous vegetables, fruits and herbs (10). Luteolin has been shown to have diverse pharmacological effects, including antioxidant, anti-inflammatory, anticancer and other biological properties (11,12). Luteolin plays a role in preventing ischemia/reperfusion injury in adult rat cardiomyocytes by improving contractile function and attenuating apoptosis (13,14), and can protect against high-carbohydrate/high-fat diet-induced myocardial inflammation through anti-inflammatory mechanisms (15). These cardiovascular protective effects of luteolin may be due to its antioxidant activities. For example, luteolin can improve angiotensin II-induced cardiac remodeling by decreasing oxidative stress (16). While increasing evidence shows that luteolin exerts cardiovascular protective effects, the possible beneficial effects of luteolin on SIC have not yet been fully clarified.

Autophagy is the main cellular pathway to maintain protein quality and organelle function, through degradation of damaged or dysfunctional cellular components (17,18). Autophagy has been shown to be involved in numerous physiological processes, such as the starvation response, cell growth control, anti-aging mechanisms and innate immunity (19). Studies have shown that autophagy is mobilized early in sepsis and is seen in various organs by an increased accumulation of autophagic vacuoles and enhanced expression of autophagy-associated proteins (9,20,21). Various kinds of drugs administered to reverse sepsis-induced immunoparalysis have been shown to be autophagy-dependent (21). AMP-activated protein kinase (AMPK) not only plays a key role in sensing the energy status and regulating cellular energy homeostasis, but is also an important positive regulator of autophagy (22). Moreover, activation of AMPK can ameliorate the organ injury induced by sepsis through decreasing inflammatory cytokine levels and endothelial activation (23).

The present study sought to demonstrate the potential effects of luteolin on lipopolysaccharide (LPS)-induced myocardial injury via increasing autophagy. Whether the protective effect of luteolin on autophagy was mediated through AMPK signaling was also explored.

Materials and methods

Experimental animals. Eight-week-old male C57BL/6 mice (n=75; weight, 25-30 g) were purchased from the Laboratory Animal Center of the Fourth Military Medical University. All experimental procedures were in accordance with the National Institutes of Health Guidelines on the Care and Use of Laboratory Animal and were approved by the Fourth Military Medical University Ethics Committee on Animal Care. All mice were maintained in a temperature-controlled room (22±2˚C) under a 12-h light/dark cycle, with relative humidity of 40-60%, and free access to food and water.

Experimental protocol. The experimental mice were randomly selected and allocated into the following 3 groups (25 mice in each group): The control group (NC), the LPS group (LPS) and the LPS + luteolin group (LPS + Lut). Before the model was induced, luteolin (10 μg/kg) (99%, Sigma-Aldrich; Merck KGaA) was dissolved in DMSO and injected intraperitoneally for 10 days into LPS + Lut group animals. NC group and the LPS group mice received an equal volume of DMSO for 10 days. The animal model of sepsis-induced cardiac dysfunction was induced on day 11 by intraperitoneal injection of LPS (10 mg/kg) (Sigma-Aldrich; Merck KGaA) dissolved in normal saline. NC group mice received an equivalent volume of normal saline on day 11. Rational doses of luteolin (10 μg/kg) and LPS (10 mg/kg) were chosen according to the literature (24,25). A total of 12 h after LPS injection, M-mode echocardiography was performed and the mice were sacrificed.

Echocardiography. Echocardiography was performed using an echocardiogram (15.0 MHz, VisualSonics Vero 2100) to measure the changes in cardiac function. Two-dimensional guided M-mode measurements of the left ventricular (LV) internal diameter were obtained from the short-axis view at the level of the papillary muscles over at least three beats and were averaged. Computer algorithms were employed to measure the left ventricular end-diastolic dimension (LVEDD), left ventricular end-systolic dimension (LVESD), left ventricular ejection fraction (LVEF) and left ventricular fraction shortening (LVFS). Millar Mikro-tip catheter transducer was used and inserted into the left ventricular cavity through the left carotid artery to measure the LV pressure. Computer algorithms and an interactive videographics program (Po-Ne-Mah Physiology Platform P3 Plus, Gould Instrument Systems) were employed to obtain the first derivative of the left ventricular pressure (±LV dp/dt max).

Determination of tissue interleukin (IL)-1β, IL-6 and tumor necrosis factor (TNF)-α activity. Heart tissue samples were rinsed and perfused with normal saline and samples were homogenized. The concentrations of IL-1β (cat. no. PI301; Beyotime Institute of Biotechnology), IL-6 (cat. no. 88-7064-77; Thermo Fisher Scientific, Inc.) and TNF-α (cat. no. BMS607-3; Thermo Fisher Scientific, Inc.) were assessed using ELISA kits, following the manufacturer's protocol. Values are expressed as pg/mg of total protein.

Transmission electron microscopy. Heart tissues were removed from the animals and quickly rinsed in PBS on wet ice. Samples removed from the left ventricular myocardium were cut into 1 mm cubes and fixed with 2% glutaraldehyde for 5 h at 4˚C. Subsequently, samples were incubated with 1% osmium tetroxide for 2 h in the dark. The samples were embedded with fresh resin for 2 h at room temperature and then cut into ultrathin sections (thickness, 50-100 nm). Uranyl acetate and lead citrate were used to stain the ultrathin sections at 37˚C, for 30 and 15 min respectively, and samples were then observed using a JEOL JEM-2000EX transmission electron microscope (JEOL, Ltd.). For an *in vitro* study, primary cardiomyocytes were collected by centrifugation at 168 x g for 10 min at room temperature and fixed with 2% glutaraldehyde for 5 h at 4˚C. The fixed cells were then stained with uranyl acetate and lead citrate at 37˚C, for 30 and 15 min respectively, and images were captured using a JEOL JEM-2000EX transmission electron microscope (JEOL, Ltd.) as described above. Random sections were imaged and analyzed by two technicians blinded to the experiment.

Determination of mitochondrial transmembrane potential ($\Delta\Psi m$). Tetrachloro-tetraethyl benzimidazol carbocyanine iodide (JC-1) was employed to evaluate the changes in $\Delta\Psi m$. Primary cardiomyocytes were cultured in disposable confocal dishes at a density of $5x10^4$ cells/dish. The cells were incubated with 5 μM JC-1 (Beyotime Institute of Biotechnology) for 30 min at 37˚C in the dark and washed twice with PBS. JC-1-labelled cells were visualized using an Olympus FV1000 laser confocal microscope. Cellular mitochondria with normal $\Delta\Psi m$ emitted red fluorescence (J-aggregate), while those with abnormal $\Delta\Psi m$ showed green fluorescence (J-monomer).

Isolation of mitochondria. Mitochondria were isolated from hearts using the Cell Mitochondria Isolation kit (Beyotime Institute of Biotechnology) as previously described (26). Isolated mitochondria were maintained on wet ice at 0˚C before downstream processing.

Measurement of citrate synthase and electron transport chain complex activities and ATP content. Citrate synthase (CS) and electron transport chain complex activities were measured using the CS Assay kit (Sigma-Aldrich; Merck KGaA) following the manufacturer's protocol. The ATP content of heart tissues was detected using an adenosine triphosphate bioluminescence assay kit (Beyotime Institute of Biotechnology).

Determination of mitochondrial calcium retention capacity (mCRC). The mCRC represents the capacity of mitochondria to take in calcium before permeability transition. The mCRC level was assessed as previously described (27).

Estimation of malondialdehyde (MDA) and reactive oxygen species (ROS) production in heart tissue. Heart tissues were weighed and homogenized (1:10, w/v) in phosphate buffer (50 mM, pH 7.4). The levels of ROS and MDA were measured using the ROS Assay kit and Lipid Peroxidation MDA assay kit according to the manufacturer's protocol (Nanjing Jiancheng Bioengineering Institute).

Western blot analysis. Cardiac tissues or cardiomyocytes were harvested and homogenized with RIPA buffer containing protease inhibitor cocktail (Roche Diagnostics) on ice. After centrifugation at 12,000 x g for 15 min at 4˚C, the total protein content of the supernatant was quantified using a bicinchoninic acid protein assay (Applygen Technologies, Inc.) and the supernatant was stored at -80˚C until use. Protein samples (40 μg protein/lane) were separated using 10% SDS-PAGE gels, transferred to polyvinylidene difluoride membrane (EMD Millipore) and incubated overnight at 4˚C with the primary antibodies. The blots were then incubated with horseradish peroxidase-conjugated secondary antibody for 1 h at 37˚C. Immunoreactive bands were detected and scanned with ECL™ Advance Western Blotting Detection kit (Amersham Bioscience). ImageJ Version 1.8.0 software (National Institutes of Health) was used to analyze protein band intensity.

Reagents and antibodies. Antibodies against the following proteins were used: Sequestosome 1 (p62; 1:1,000; cat. no. ab109012; Abcam), Beclin1 (1:1,000; cat. no. ab210498; Abcam), cleaved caspase-3 (1:1,000; cat. no. AB3623; Sigma-Aldrich; Merck KGaA), cleaved caspase-9 (1:1,000; cat. no. AB3629; Sigma-Aldrich; Merck KGaA), microtubule-associated protein light chain 3 A/B (LC3A/B; 1:1,000; cat. no. 4108; Cell Signaling Technology, Inc.), AMPK (1:1,000; cat. no. 5831; Cell Signaling Technology, Inc.), phosphorylated (p)-AMPK (Thr172) (1:1,000; cat. no. 2535; Cell Signaling Technology, Inc.), Unc-51 like autophagy activating kinase 1 (ULK1; 1:1,000; cat. no. 6439; Cell Signaling Technology, Inc.), p-ULK1 (Ser757) (1:1,000; cat. no. 14202; Cell Signaling Technology, Inc.) and β-actin (1:5000; cat. no. sc-47778; Santa Cruz, Biotechnology. Inc.). Horseradish peroxidase-conjugated secondary antibodies (anti-mouse/rabbit IgG) (1:5,000; cat. nos. 7076 and 7074; Cell Signaling Technology, Inc.) were used.

Culture of neonatal mouse ventricular cardiomyocytes. Isolation of primary neonatal mouse cardiomyocytes was described previously (26). Male C57BL/6 mice (n=60; age, 1-day-old; weight, 1.5-3 g) were purchased from the Laboratory Animal Center of the Fourth Military Medical University. Neonatal mice were sacrificed and hearts were quickly excised and minced into fragments prior to enzymatic digestion with collagenase type 2 (Sigma-Aldrich; Merck KGaA). After digestion for several minutes, the digested fragments were placed on a sterilized platform to sediment for several minutes and digested cells in supernatants were pre-plated for 1 h to remove fibroblasts and endothelial cells. The residual supernatant with abundant cardiomyocytes (10,000-12,000 cells/cm^2) was re-plated in DMEM (Gibco; Thermo Fisher Scientific, Inc.) supplemented with 20% fetal bovine serum (Gibco; Thermo Fisher Scientific, Inc.) and 1% penicillin-streptomycin at 37˚C in 95% O_2 and 5% CO_2. On the fourth day after isolation, spontaneous beating of the primary neonatal mouse cardiomyocytes was observed. Troponin T (cTnT) is a marker specific to cardiomyocytes. A monoclonal antibody against cTnT (1:200; cat. no. sc-20025; Santa Cruz Biotechnology, Inc.) was used to identify the primary neonatal mouse cardiomyocytes (data not shown). To determine whether luteolin could protect cardiomyocytes against LPS-induced injury, cardiomyocytes were pretreated with luteolin in the absence or presence of LPS. Luteolin (20 μM) was added to the medium for 6 h and cells were then exposed to LPS (10 μg/ml) for 24 h. Cells were also pretreated with the AMPK activator 5-aminoimidazole-4-carboxamide ribonucleotide (AICAR; 1 mM), the autophagy inhibitor 3-methyladenine (3-MA; 10 mM), or the AMPK inhibitor dorsomorphin (compound C, CC, 10 mM) to evaluate the changes in protein expression and autophagic activity.

Determination of cardiomyocyte apoptosis. A TUNEL assay kit (*In Situ* Cell Death Detection kit; Roche Diagnostics) was used to measure the apoptosis ratio of the cardiomyocytes as described previously (26). TUNEL was performed with fluorescein-dUTP for 1 h at 37˚C to identify apoptotic cell nuclei and 4',6-diamidino-2-phenylindole (DAPI; Sigma-Aldrich; Merck KGaA) was used to stain all cell nuclei for 5 min at room temperature. A monoclonal antibody against cTnI (Santa Cruz Biotechnology, Inc.) was used to stain and identify the myocardium. The apoptotic index was calculated as the ratio of TUNEL-positive cells to the total number of DAPI-positive cells within the same area from five randomly selected fields in each group.

Statistical analysis. All tests were repeated three times. Continuous variables are presented as means ± standard error of the mean. Differences between specific groups were determined by one-way analysis of variance followed by the Student-Newman-Keuls test. $P<0.05$ was considered to indicate a statistically significant difference. SPSS software package version 14.0 (SPSS, Inc.) was used for data analysis.

Results

Luteolin improves cardiac function in mice with LPS-induced sepsis. To investigate the effect of luteolin treatment on cardiac function in mice with sepsis, echocardiography was used to assess cardiac function parameters (Fig. 1A). LVEDD and LVESD were significantly increased in the LPS group compared with the control group. Luteolin treatment significantly suppressed the increases in LVEDD and LVESD in

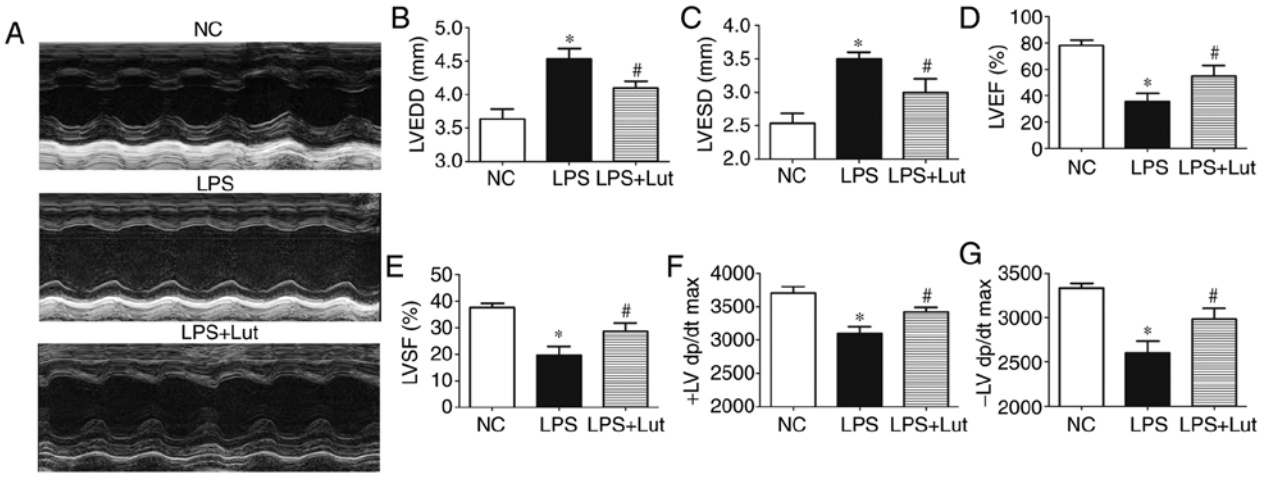

Figure 1. Effects of Lut on cardiac function in LPS-induced septic mice. (A) Representative echocardiographic images are shown. (B) LVEDD. (C) LVESD. (D) LVEF. (E) LVFS. First (F) + and (G) -LV dp/dt max. The columns and error bars represent the means and standard error of the mean (n=10). *P<0.05 vs. NC; #P<0.05 vs. LPS. LVEDD, left ventricular end-diastolic diameter; LVESD, left ventricular end-systolic diameter; LVEF, left ventricular ejection fraction; LVFS, left ventricular fraction shortening; LPS, lipopolysaccharide; NC, negative control; ±LV dp/dt max, derivative of the left ventricular pressure; Lut, luteolin.

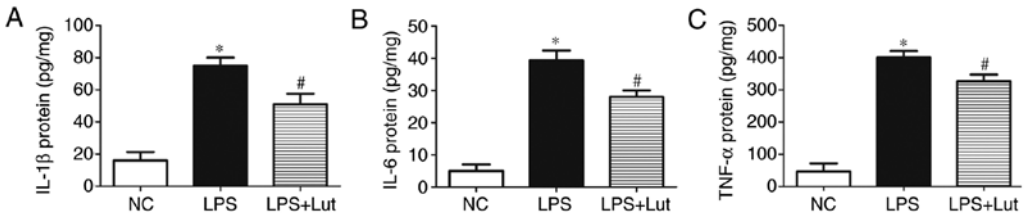

Figure 2. Effects of Lut on the inflammatory response in LPS-induced septic mice. Lut decreased the levels of (A) IL-1β, (B) IL-6 and (C) TNF-α in septic heart tissue. The columns and error bars represent the means and standard error of the mean (n=5). *P<0.05 vs. NC; #P<0.05 vs. LPS. IL, interleukin; TNF-α, tumor necrosis factor-α; LPS, lipopolysaccharides; NC, negative control; Lut, luteolin.

mice with sepsis compared with the LVEDD and LVESD in untreated mice with sepsis (Fig. 1B and C). LVEF, LVFS, and ±LV dp/dt were decreased in the LPS group compared with in the control group. Treatment with luteolin increased the LVEF, LVFS and ± LV dp/dt values in mice with sepsis compared with those in untreated mice with sepsis (Fig. 1D-G).

Luteolin attenuates inflammation in the hearts of septic mice. Further experiments were done to examine the effects of luteolin treatment on the inflammatory response in septic hearts. The levels of the inflammatory factors IL-1β, IL-6 and TNF-α were increased in the septic myocardium compared with in the control myocardium. In contrast, lower levels of IL-1β, IL-6 and TNF-α were detected in the LPS + luteolin group compared with in the LPS group (Fig. 2-C).

Luteolin decreases cardiac apoptosis in mice with LPS-induced sepsis. A TUNEL assay was performed to evaluate the effects of luteolin on cardiac apoptosis (Fig. 3A). Significantly more TUNEL-positive cardiomyocytes were detected in the LPS group than in the control group, but this was attenuated by luteolin treatment (Fig. 3B). Western blotting was used to assess caspase enzyme activity (Fig. 3C). The levels of cleaved caspase-3 and cleaved caspase-9 were significantly increased in the LPS group compared with in the control group, but luteolin treatment decreased these levels in the myocardium of septic mice (Fig. 3D and E).

Luteolin attenuates mitochondrial injury and oxidative stress in the hearts of septic mice. Mitochondrial dysfunction is correlated with the deterioration of myocardial function during sepsis. Transmission electron microscopy (TEM) was used to evaluate the effect of luteolin treatment on mitochondrial ultrastructural changes in mice with sepsis (Fig. 4A). Normal mitochondria with organized cristae packed beside symmetric myofibrils were seen in the hearts of control mice. In the myocardium of septic mice, the mitochondria were swollen and disarranged. In addition, rarefaction and vacuolization of the mitochondrial structure, as well as rupture and disappearance of the mitochondrial cristae, were seen. In the LPS + Lut group, most mitochondria displayed sharply defined cristae. The ATP content, CS activity and complex I/II/III/IV/V activities in the isolated mitochondria were significantly decreased in the LPS group compared with those in the control group and these activities were enhanced in the LPS + Lut group (Fig. 4B, C and D). The mCRC, determined as the capacity of mitochondria to uptake calcium before permeability transition, was used to assess the sensitivity of mitochondrial permeability transition pore (mPTP) opening to calcium (Fig. 4E). The mCRC was significantly decreased in the LPS group compared with in the control group. However, treatment with luteolin significantly increased the mCRC, indicating that the sensitivity to calcium-induced mPTP opening was decreased.

Oxidative stress contributes to myocardial injury during sepsis. The ROS and MDA levels were measured to explore

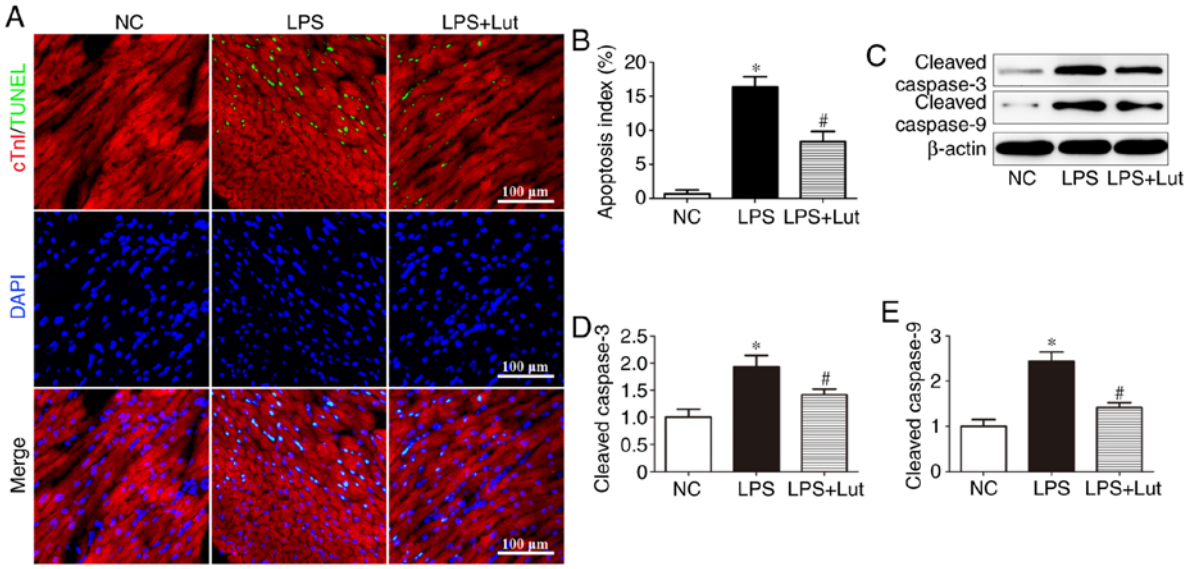

Figure 3. Effects of Lut on cardiac apoptosis in LPS-induced septic mice. (A) Representative immunofluorescence images of TUNEL (green), DAPI staining (blue) and cTnI antibody staining (red) and (B) quantification of TUNEL-positive cells. The columns and error bars represent the means and SEMs (n=5). *P<0.05 vs. NC; #P<0.05 vs. LPS. Representative (C) immunoblots of protein expression levels in the myocardium, with quantitative analysis for cleaved (D) caspase-3, (E) cleaved caspase-9 and β-actin. The columns and error bars represent the means and SEMs (n=5). *P<0.05 vs. NC; #P<0.05 vs. LPS. cTnI, Troponin I; LPS, lipopolysaccharides; SEM, standard error of the mean; DAPI, 4',6-diamidino-2-phenylindole; TUNEL, terminal deoxynucleotidyl-transferase-mediated dUTP nick end labelling; NC, negative control; Lut, luteolin.

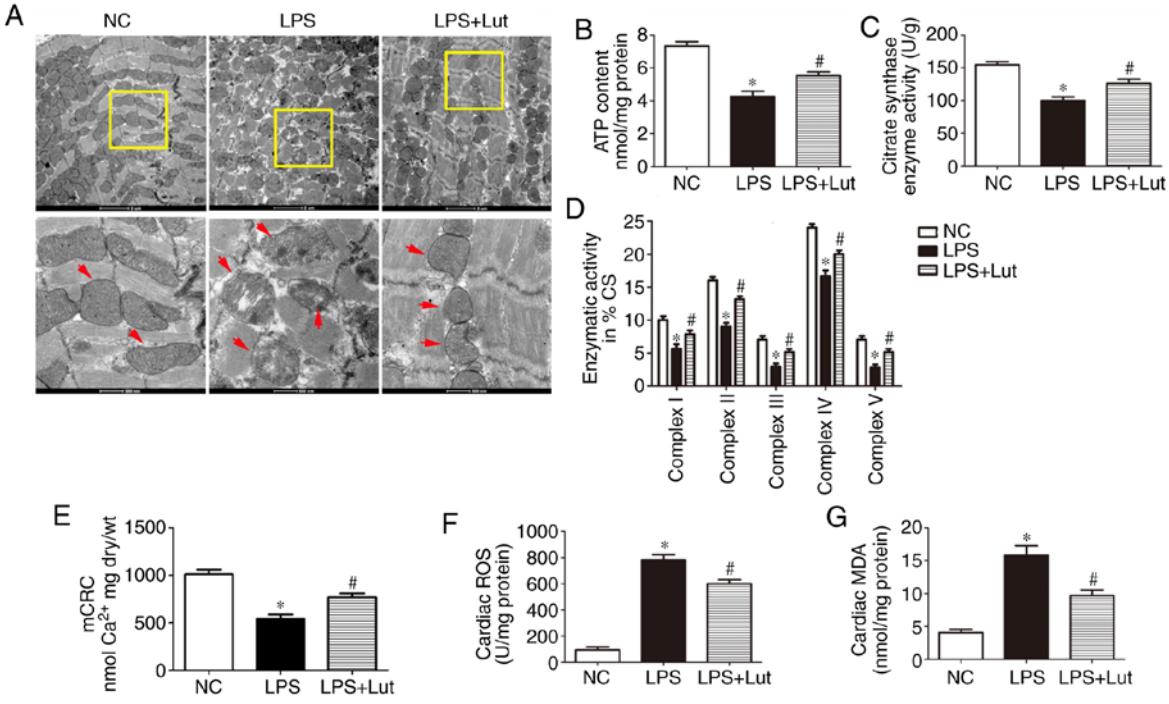

Figure 4. Effects of Lut on mitochondrial function in LPS-induced septic mice. (A) Representative transmission electron micrographs of left ventricular specimens (magnification, x8,200 and x26,500, the red arrows indicate mitochondria). (B) ATP content and (C) CS and (D) complex I/II/III/IV/V activities in mitochondria isolated from mice. (E) mCRC. (F) ROS and (G) MDA levels. The columns and error bars represent the means and standard error of the mean (n=5). *P<0.05 vs. NC; #P<0.05 vs. LPS. LPS, lipopolysaccharides; MDA, malondialdehyde; NC, negative control; mCRC, mitochondrial calcium retention capacity; CS, citrate synthase; ROS, reactive oxygen synthase; Lut, luteolin.

the effect of luteolin treatment on oxidative stress in septic heart tissue. The levels of ROS and MDA were significantly enhanced in the LPS group compared with in the control group and luteolin administration significantly inhibited these increases (Fig. 4F and G).

Luteolin enhances autophagy through AMPK activation in the hearts of septic mice. Impairment of autophagy may contribute to contractile dysfunction and apoptotic cardiomyocyte death in sepsis. As shown by TEM, more autophagosomes were observed in the LPS group compared

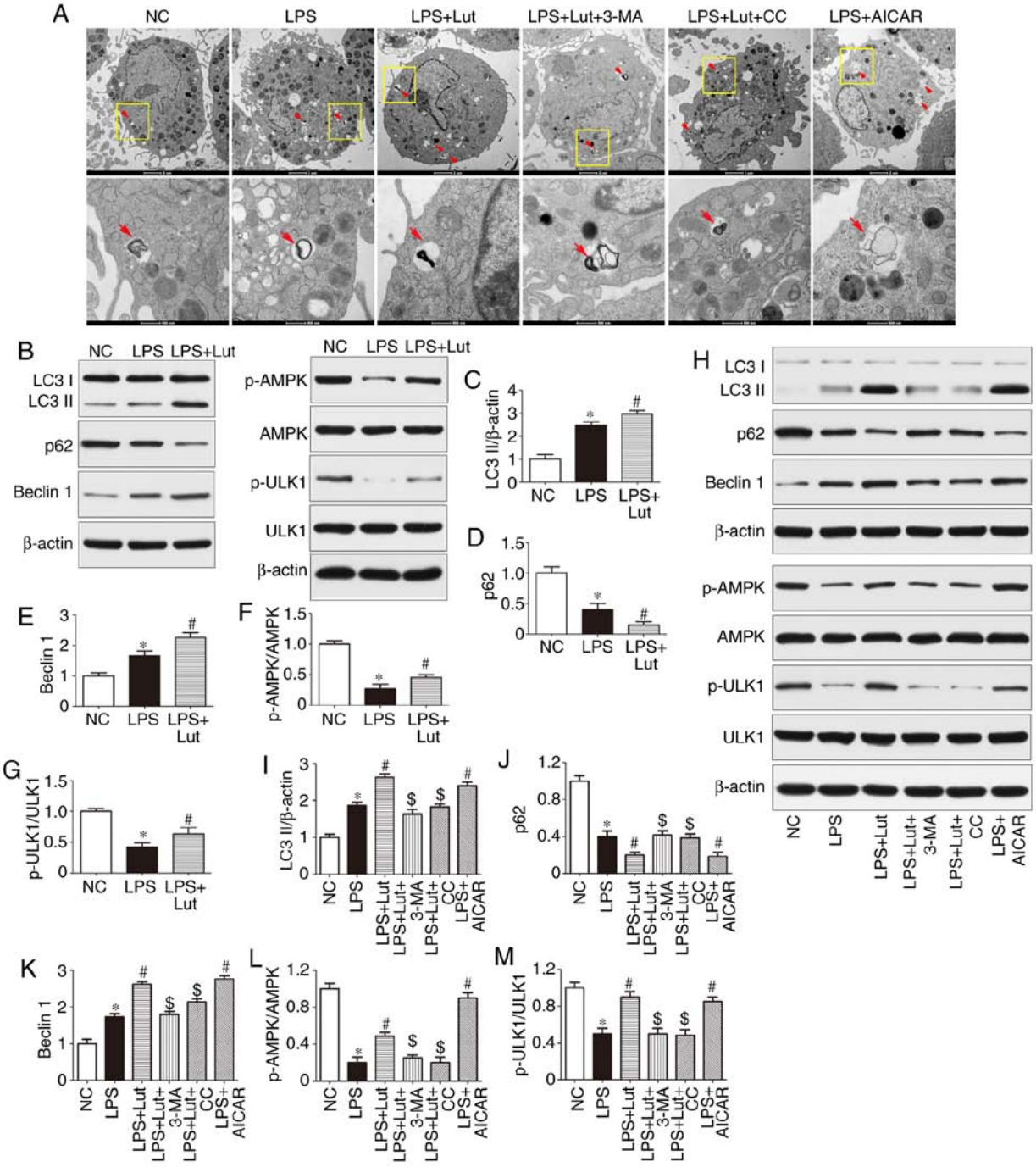

Figure 5. Effects of Lut on autophagy in the hearts of septic mice and in LPS-treated cardiomyocytes. (A) Representative images of ultrastructural morphology and typical autophagosomes in cardiomyocytes subjected to different treatments (magnification, x6,000 and x43,000, the red arrows indicate autophagosomes). (B) Representative immunoblots and densitometric quantification for (C) LC3II, (D) P62, (E) Beclin1, (F) p-AMPK, AMPK, (G) p-ULK1, ULK1, and β-actin in myocardial tissues from the indicated groups. The columns and error bars represent the means and SEMs (n=5). *P<0.05 vs. NC; $^{\#}$P<0.05 vs. LPS. (H) Representative immunoblots and densitometric quantification for (I) LC3II, (J) P62, (K) Beclin1, (L) p-AMPK, AMPK, (M) p-ULK1, ULK1, and β-actin in cardiomyocytes from the indicated groups. The columns and error bars represent the means and SEMs. *P<0.05 vs. NC; $^{\#}$P<0.05 vs. LPS; $^{\$}$P<0.05 vs. LPS + Lut. p62, sequestosome 1; LC3II, microtubule-associated protein light chain 3II; AMPK, AMP-activated protein kinase; ULK1, Unc-51 like autophagy activating kinase 1; 3-MA, 3-methyladenine; AICAR, 5-aminoimidazole-4-carboxamide ribonucleotide; CC, dorsomorphin, compound C; p-, phosphorylated; SEM, standard error of the mean; NC, negative control; Lut, luteolin.

with in the control group. Luteolin further increased the number of autophagosomes in septic mice (Fig. 5A). Western blotting was used to assess autophagic activity in the hearts of septic mice and in LPS-treated cardiomyocytes (Fig. 5B and H). The expression of LC3 II and Beclin1 was increased and that of p62 was lower in the hearts of septic mice than in the hearts of control mice. However, luteolin treatment further increased LC3-II and Beclin1 expression and decreased p62 expression in septic mice (Fig. 5B-E). The effect of luteolin on LC3-II, p62 and Beclin1 expression in LPS-treated cardiomyocytes was consistent with the *in vivo* effect (Fig. 5H-K). In addition, the autophagy inhibitor 3-MA abolished the effect of luteolin on autophagic activity in cardiomyocytes (Fig. 5H-K).

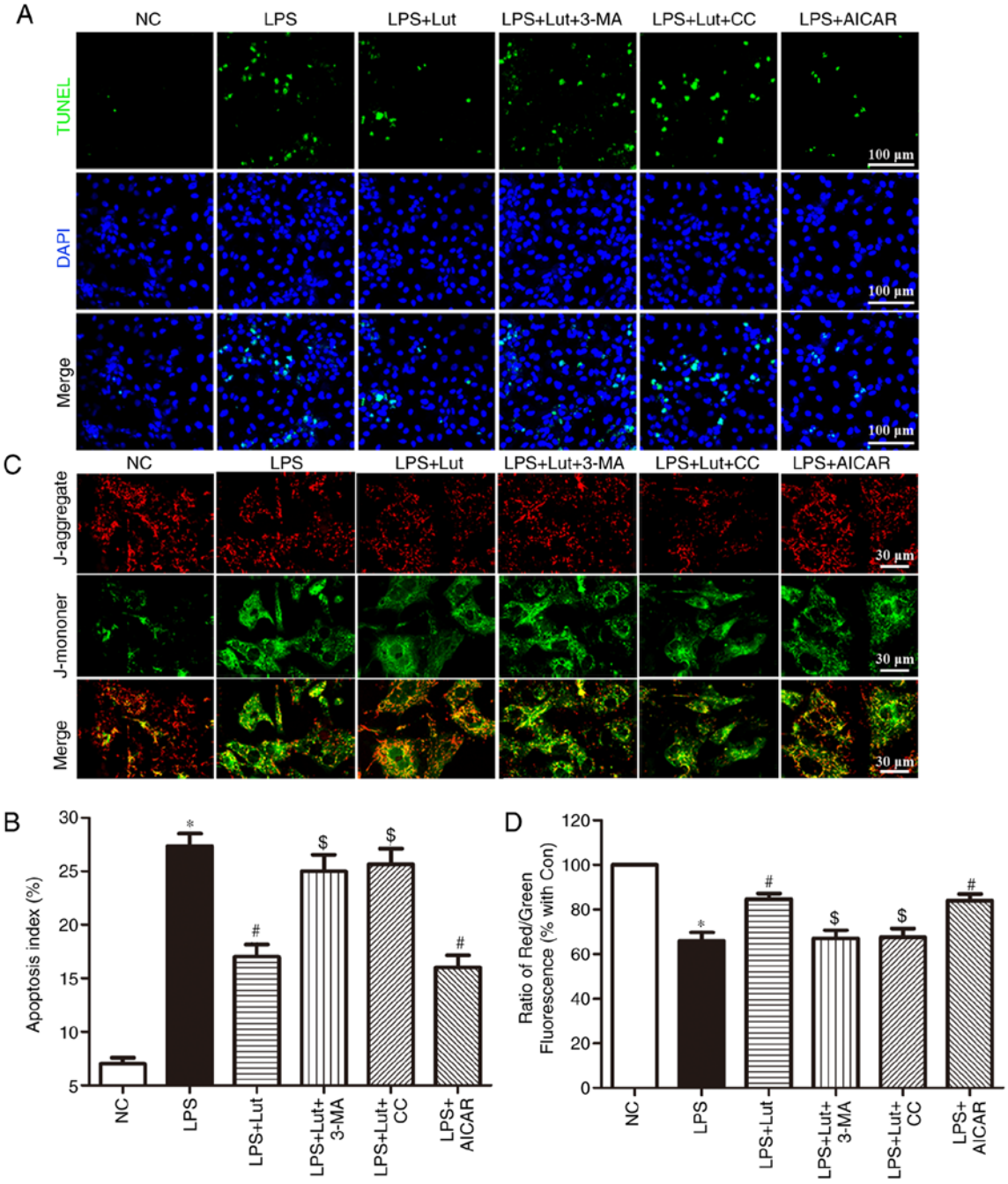

Figure 6. Effects of Lut on apoptosis and mitochondrial transmembrane potential in LPS-treated cardiomyocytes. (A) Representative images of the TUNEL assay in primary neonatal cardiomyocytes and (B) quantitative analysis of the apoptotic index. (C) Representative images of JC-1 staining in cardiomyocytes. (D) The ratio of aggregated and monomeric JC-1. The columns and error bars represent the means and standard error of the mean. *P<0.05 vs. NC; #P<0.05 vs. LPS; $P<0.05 vs. LPS + Lut. 3-MA, 3-methyladenine; AICAR, 5-aminoimidazole-4-carboxamide ribonucleotide; CC, dorsomorphin, compound C; LPS, lipopolysaccharide; NC, negative control; Lut, luteolin; TUNEL, terminal deoxynucleotidyl-transferase-mediated dUTP nick end labeling.

Western blotting was used to measure the expression of AMPK signaling proteins (Fig. 5B and H). The phosphorylation of AMPK and ULK1 was reduced in the hearts of septic mice compared with control mice and luteolin enhanced the phosphorylation of AMPK and ULK1 in the hearts of septic mice (Fig. 5B, F, and G). Similar effects were found *in vitro* (Fig. 5H, L and M). More notably, the AMPK inhibitor compound C abolished the effect of luteolin on autophagic activity in LPS-treated cardiomyocytes, as evidenced by the decrease in LC3 II and Beclin1 expression and the increase in p62 expression, while the AMPK activator AICAR mimicked the effect of luteolin in LPS-treated cardiomyocytes (Fig. 5H-K).

Luteolin inhibits apoptosis in LPS-treated cardiomyocytes. A TUNEL assay was employed to assess the effects of luteolin on apoptosis in LPS-treated cardiomyocytes (Fig. 6A). Consistent with the *in vivo* effect, luteolin treatment inhibited LPS-induced cardiomyocyte apoptosis. Interestingly, 3-MA and compound C reversed the anti-apoptotic effect of luteolin in LPS-treated cardiomyocytes, while AICAR appreciably emulated the effect of luteolin (Fig. 6A and B).

Luteolin stabilizes the mitochondrial transmembrane potential in LPS-treated cardiomyocytes. Stability of the mitochondrial membrane potential is helpful for maintaining the normal physiological function of cardiomyocytes. LPS harms mitochondria and results in the loss of mitochondrial membrane potential. JC-1 was employed to measure the changes in the mitochondrial transmembrane potential (Fig. 6C). A decrease in the mitochondrial membrane potential was noted in LPS-treated cardiomyocytes compared with that in control cardiomyocytes. Luteolin treatment enhanced the mitochondrial membrane potential in LPS-induced cardiomyocytes. Notably, this effect of luteolin was abolished by 3-MA and compound C but was mimicked by AICAR (Fig. 6C and D).

Discussion

The major finding in the present study is that luteolin treatment ameliorates LPS-induced myocardial injury by increasing autophagy via AMPK signaling. The protective effects of luteolin against SIC were associated with restored cardiac function, reduced inflammation, ameliorated mitochondrial injury, inhibited cardiac apoptosis and enhanced cardiac autophagy in septic mice, and AMPK signaling was strongly involved in these protective effects. In the present study, the cardioprotective effect of luteolin against SIC was underscored by reduced levels of the inflammatory cytokines IL-1β, IL-6 and TNF-α, as well as the decrease in cardiac apoptosis in both *in vitro* and *in vivo* models. Moreover, luteolin increased autophagic activity in the hearts of septic mice. However, this action of luteolin was abolished by 3-MA in cardiomyocytes treated with LPS, suggesting that autophagy may be essential for luteolin to maintain cardiac structure and function in response to sepsis. In addition, luteolin treatment enhanced the phosphorylation of AMPK and ULK1 in LPS-treated cardiomyocytes, while inhibition of AMPK by compound C abolished the protective effect of luteolin and significantly decreased autophagic activity in cardiomyocytes treated with LPS, indicating the association between the protective effects of luteolin, autophagic activity, and AMPK signaling activation.

Increasing evidence has demonstrated that luteolin has a certain therapeutic effect on cardiovascular disease, including preventing ischemia/reperfusion injury in adult rats (14) and sodium fluoride-induced hypertension in rats (28), ameliorating inorganic mercury-induced cardiac injury in rats (29), decreasing high-carbohydrate/high-fat diet-induced myocardial inflammation (15), and improving angiotensin II-induced cardiac remodeling by decreasing oxidative stress (16). SIC, first described by Parker *et al* (30) in 1984, is a complication of severe sepsis and septic shock characterized by an invertible myocardial depression. LV dilatation and decreased ejection fraction as measured by echocardiography are the major hemodynamic characteristics of SIC (31). The possible beneficial effects of luteolin on SIC have not yet been fully demonstrated. In the present study, treatment with luteolin increased the LVEF, LVFS and ±LV dp/dt values and decreased the LVEDD and LVESD values in mice with sepsis. The present study to the best of our knowledge, is the first to report that cardiac function was improved by luteolin administration in septic mice.

The inflammatory response is the initial process in and the hallmark of SIC development (7). In response to infection, pro-inflammatory and anti-inflammatory mediators are released (32). Excessive levels of pro-inflammatory mediators result in the inflammatory response that characterizes sepsis, while the compensatory anti-inflammatory reaction fails to suppress the immune response (32). TNF-α, IL-1 and IL-6 are the main inflammatory mediators that lead to myocardial depression in sepsis (33). Antonucci *et al* (34) argued that the interaction between TNF-α/IL-1 and inducible nitric oxide synthase exerts a negative inotropic effect on the septic myocardium. Pathan *et al* (35) showed that IL-6 contributed to myocardial depression manifested as induced cardiac contractile dysfunction and inotrope insensitivity due to the dysregulation of p38 mitogen-activated protein kinase signaling. Vincent *et al* (36) reported that treatment with anti-TNF antibodies improved LV function in patients with septic shock. In the present study, the levels of the inflammatory factors IL-1β, IL-6 and TNF-α were increased in the septic myocardium, consistent with previous findings (33-36). Moreover, the current study found that luteolin treatment attenuated inflammation in the hearts of septic mice, suggesting that the cardioprotective effects of luteolin are related to its anti-inflammatory activity in septic mice.

Structural injury and functional impairment of mitochondria play an important role in the pathogenesis of sepsis, and the degree of mitochondrial injury is related to prognosis (8). The decrease in the mitochondrial membrane potential concurrent with the release of hydrogen peroxide has been documented in experimental sepsis (37-39). In addition, mitochondria-generated ROS may serve as signaling molecules to communicate with other cellular compartments (40). Mitochondrial impairment could contribute to oxidative stress in the septic myocardium, leading to myocardial injury (40). The present study revealed mitochondrial ultrastructural damage in the hearts of septic mice. Luteolin treatment ameliorated the pathological abnormalities of mitochondria in septic mice, as evidenced by the sharply defined cristae in the hearts of septic mice. Moreover, luteolin enhanced the ATP content, CS activity, complex I/II/III/IV/V activities and mCRC in LPS-treated mice and increased the mitochondrial membrane potential in LPS-treated cardiomyocytes. Simultaneously, luteolin administration inhibited the increases in ROS and MDA levels in septic heart tissue. These results indicate that the effects of luteolin against SIC may be associated with antioxidant activity.

Apoptosis has been extensively implicated as a determining process in sepsis-induced myocardial depression (41). Cellular damage, such as cardiomyocyte apoptosis and upregulated caspase activity, was observed in the septic myocardium, while caspase inhibition ameliorated cardiac function and apoptosis in the hearts of septic rats (41). In the present study, luteolin treatment decreased the percentage of TUNEL-positive cardiomyocytes both in the hearts of septic mice and in LPS-treated cells. In addition, the expression of caspase enzymes was measured to demonstrate the molecular basis of the effects of luteolin. Luteolin treatment attenuated the expression of cleaved caspase-3 and cleaved caspase-9 in the myocardium of septic mice. These data indicate that caspase inhibition may be involved in the anti-apoptotic effect of luteolin in the hearts of septic mice.

Autophagy is an important self-protective mechanism, promoting cellular survival by controlling the degradation of proteins and organelles, including the formation of double-membraned autophagosomes and proteolytic degradation after delivery to lysosomes (21,42). This process is the primary mechanism for mitochondrial quality control, preventing apoptosis and promoting antigen presentation (9), and dysregulation has been shown to have significant harmful effects on the heart (42). Activation of autophagy has been observed in a variety of heart diseases, including cardiac hypertrophy and ischemia/reperfusion injury, suggesting that autophagy may play an important role in myocardial dysfunction (43). Previous *in vitro* and *in vivo* models of sepsis showed that autophagy was initially activated in sepsis, followed by a subsequent phase of impairment (9,44). Incomplete activation of autophagy may contribute to cardiac dysfunction during sepsis (44). In the present study, autophagic activity was upregulated in the hearts of septic mice and in LPS-treated cardiomyocytes, as revealed by the increased expression of LC3II and Beclin1, decreased expression of p62, and accumulation of autophagosomes, consistent with previous studies (9,44). Moreover, autophagy modulation appears to be protective against myocardial injury in murine sepsis models (9,44). Multiple drugs and bioactive molecules exerting cardioprotective effects in sepsis are correlated with the regulation of autophagy (44). Rapamycin, an autophagy inducer, exerts a cardioprotective effect in sepsis through the complete induction of autophagy (44). P27, a canonical tumor suppressor, protects cardiomyocytes from sepsis-induced cardiac depression via the activation of autophagy and inhibition of apoptosis (45). In addition, luteolin regulates autophagy in numerous other circumstances, including attenuation of post-infarction cardiac dysfunction (25) and decreasing foam cell formation and apoptosis in ox-LDL-stimulated macrophages by enhancing autophagy (46), and promoting apoptosis by inducing autophagy in hepatocellular carcinoma (47). In the current study, luteolin administration enhanced autophagy, as demonstrated by the further increase in the expression of LC3II and Beclin1 and the further decrease in the expression of p62 *in vivo* and *in vitro*, as well as by the increased number of autophagosomes in LPS-treated cardiomyocytes. It is worth noting that treatment with the autophagy inhibitor 3-MA reversed the luteolin-induced upregulation of autophagy, accompanied by decreased mitochondrial membrane potential and increased cardiomyocyte apoptosis, indicating that luteolin treatment may exert protective effects in sepsis by increasing autophagy.

AMPK is a central metabolic sensor in all eukaryotes that monitors glucose and lipid metabolism in response to changes in nutrient and intracellular energy levels (48,49). AMPK, together with ULK1, plays a vital role in promoting autophagy under nutrient or energy stress conditions, including sepsis (50,51). AMPK directly activates ULK1 through the phosphorylation of Ser 317 and Ser 777 to facilitate autophagy (22). In addition, luteolin regulates AMPK signaling in numerous other circumstances, including enhancing the survival of human umbilical vein endothelial cells against oxidative stress by modulating AMPK/protein kinase C pathway (52), improving atherosclerosis in mice via regulating AMPK/sirtuin1 signaling in macrophages (53) and reducing obesity-associated insulin resistance in mice by activating AMPK signaling in adipose tissue macrophages (54). In the present study, notably, the protective effect of luteolin was also abolished by the AMPK inhibitor compound C, as demonstrated by the decreased LC3 II and Beclin1 expression, enhanced p62 expression, destabilized mitochondrial membrane potential, and increased cardiomyocyte apoptosis. However, this effect was correspondingly mimicked by the AMPK activator AICAR in LPS-treated cardiomyocytes, suggesting that luteolin attenuates LPS-induced myocardial injury by increasing autophagy through AMPK/ULK1 signaling. The present study shows that AMPK/ULK1 signaling is involved in the role of controlling autophagy blunted in LPS-treated cardiomyocytes. Pharmacological activation of AMPK signaling improves cardiac function in mice with LPS-induced sepsis. To modulate autophagy, AMPK signaling might be a potential novel therapeutic target for septic myocardial dysfunction. In the present study, AICAR appreciably emulated the effect of luteolin in LPS-treated cardiomyocytes, also suggesting that luteolin can be used as an AMPK inducer to attenuate myocardial injury in mice with LPS-induced sepsis.

However, there are still some limitations in this study. Firstly, no control + luteolin group was set in this study. Although it has been reported that luteolin has no myocardial toxicity in normal mice (14,25), the lack of control + luteolin group makes the study design incomplete. Secondly, primary neonatal mouse cardiomyocytes were used in the *in vitro* experiment. Some primary neonatal mouse cardiomyocytes have differentiation and proliferation function, while the adult mouse cardiomyocytes belong to terminal differentiation cells and have no differentiation and proliferation function. The primary neonatal mouse cardiomyocytes can't fully mimic the adult cardiomyocytes. These problems should be considered and solved in future experiments.

In conclusion, the present study confirms that luteolin is a potential therapeutic agent for the treatment of SIC. The protective effects of luteolin against SIC may be associated with its pharmacological activities, including its antioxidant and anti-inflammatory activities. The cardioprotective effects of luteolin against SIC may also be attributed to decreasing apoptosis and enhancing autophagy through the activation of AMPK signaling. These findings may provide a promising and innovative therapeutic strategy for SIC.

Acknowledgements

Not applicable.

Funding

The present study was supported by the National Natural Science Foundation of China (grant no. 81200189), the Shaanxi Social Development and Scientific Program Tackling Program (grant no. 2016SF021) and the New Technology Foundation of Xijing Hospital (grant no. 2016-15).

Availability of data and materials

The data generated or analyzed during this study are included in this published article.

Authors' contributions

BW and MY made substantial contributions to the conception and design of the experiments. BW, HS, MF, FY, LZ, JL, JL, LW and CL conducted the experiments. BW, HS, and MF analyzed the experimental data and wrote the manuscript. MY edited and revised the manuscript. All authors read and approved the final manuscript.

Ethics approval and consent to participate

All experimental procedures were in accordance with the National Institutes of Health Guidelines on the Care and Use of Laboratory Animal and were approved by the Fourth Military Medical University Ethics Committee on Animal Care.

Patient consent for publication

Not applicable.

Competing interests

The authors declare that they have no competing interests.

References

1. Singer M, Deutschman CS, Seymour CW, Shankar-Hari M, Annane D, Bauer M, Bellomo R, Bernard GR, Chiche JD, Coopersmith CM, *et al*: The third international consensus definitions for sepsis and septic shock (Sepsis-3). JAMA 315: 801-810, 2016.
2. Mayr FB, Yende S and Angus DC: Epidemiology of severe sepsis. Virulence 5: 4-11, 2014.
3. Plevin R and Callcut R: Update in sepsis guidelines: What is really new? Trauma Surg Acute Care Open 2: e000088, 2017.
4. Cheng B, Hoeft AH, Book M, Shu Q and Pastores SM: Sepsis: Pathogenesis, biomarkers, and treatment. Biomed Res Int 2015: 846935, 2015.
5. Maloney PJ: Sepsis and septic shock. Emerg Med Clin North Am 31: 583-600, 2013.
6. Adhikari NK, Fowler RA, Bhagwanjee S and Rubenfeld GD: Critical care and the global burden of critical illness in adults. Lancet 376: 1339-1346, 2010.
7. Kakihana Y, Ito T, Nakahara M, Yamaguchi K and Yasuda T: Sepsis-induced myocardial dysfunction: Pathophysiology and management. J Intensive Care 4: 22, 2016.
8. Liu YC, Yu MM, Shou ST and Chai YF: Sepsis-induced cardiomyopathy: mechanisms and treatments. Front Immunol 8: 1021, 2017.
9. Ho J, Yu J, Wong SH, Zhang L, Liu X, Wong WT, Leung CC, Choi G, Wang MH, Gin T, *et al*: Autophagy in sepsis: Degradation into exhaustion? Autophagy 12: 1073-1082, 2016.
10. Luo Y, Shang P and Li D: Luteolin: A flavonoid that has multiple cardio-protective effects and its molecular mechanisms. Front Pharmacol 8: 692, 2017.
11. Lopez-Lazaro M: Distribution and biological activities of the flavonoid luteolin. Mini Rev Med Chem 9: 31-59, 2009.
12. Seelinger G, Merfort I and Schempp CM: Anti-oxidant, anti-inflammatory and anti-allergic activities of luteolin. Planta Med 74: 1667-1677, 2008.
13. Xu T, Li D and Jiang D: Targeting cell signaling and apoptotic pathways by luteolin: Cardioprotective role in rat cardiomyocytes following ischemia/reperfusion. Nutrients 4: 2008-2019, 2012.
14. Qi L, Pan H, Li D, Fang F, Chen D and Sun H: Luteolin improves contractile function and attenuates apoptosis following ischemia-reperfusion in adult rat cardiomyocytes. Eur J Pharmacol 668: 201-207, 2011.
15. Abu-Elsaad N and El-Karef A: The falconoid luteolin mitigates the myocardial inflammatory response induced by high-carbohydrate/high-fat diet in wistar rats. Inflammation 41: 221-231, 2018.
16. Nakayama A, Morita H, Nakao T, Yamaguchi T, Sumida T, Ikeda Y, Kumagai H, Motozawa Y, Takahashi T, Imaizumi A, *et al*: A food-derived flavonoid luteolin protects against angiotensin II-induced cardiac remodeling. PLoS One 10: e0137106, 2015.
17. Parzych KR and Klionsky DJ: An overview of autophagy: Morphology, mechanism, and regulation. Antioxid Redox Signal 20: 460-473, 2014.
18. Mialet-Perez J and Vindis C: Autophagy in health and disease: Focus on the cardiovascular system. Essays Biochem 61: 721-732, 2017.
19. Morel E, Mehrpour M, Botti J, Dupont N, Hamai A, Nascimbeni AC and Codogno P: Autophagy: A druggable process. Annu Rev Pharmacol Toxicol 57: 375-398, 2017.
20. Takahashi W, Watanabe E, Fujimura L, Watanabe-Takano H, Yoshidome H, Swanson PE, Tokuhisa T, Oda S and Hatano M: Kinetics and protective role of autophagy in a mouse cecal ligation and puncture-induced sepsis. Crit Care 17: R160, 2013.
21. Ren C, Zhang H, Wu TT and Yao YM: Autophagy: A potential therapeutic target for reversing sepsis-induced immunosuppression. Front Immunol 8: 1832, 2017.
22. Kim J, Kundu M, Viollet B and Guan KL: AMPK and mTOR regulate autophagy through direct phosphorylation of Ulk1. Nat Cell Biol 13: 132-141, 2011.
23. Escobar DA, Botero-Quintero AM, Kautza BC, Luciano J, Loughran P, Darwiche S, Rosengart MR, Zuckerbraun BS and Gomez H: Adenosine monophosphate-activated protein kinase activation protects against sepsis-induced organ injury and inflammation. J Surg Res 194: 262-272, 2015.
24. Li P, Chen XR, Xu F, Liu C, Li C, Liu H, Wang H, Sun W, Sheng YH and Kong XQ: Alamandine attenuates sepsis-associated cardiac dysfunction via inhibiting MAPKs signaling pathways. Life Sci 206: 106-116, 2018.
25. Hu J, Man W, Shen M, Zhang M, Lin J, Wang T, Duan Y, Li C, Zhang R, Gao E, *et al*: Luteolin alleviates post-infarction cardiac dysfunction by up-regulating autophagy through Mst1 inhibition. J Cell Mol Med 20: 147-156, 2016.
26. Wu B, Lin J, Luo J, Han D, Fan M, Guo T, Tao L, Yuan M and Yi F: Dihydromyricetin protects against diabetic cardiomyopathy in streptozotocin-induced diabetic mice. Biomed Res Int 2017: 3764370, 2017.
27. Zhang M, Wang C, Hu J, Lin J, Zhao Z, Shen M, Gao H, Li N, Liu M, Zheng P, *et al*: Notch3/Akt signaling contributes to OSM-induced protection against cardiac ischemia/reperfusion injury. Apoptosis 20: 1150-1163, 2015.
28. Oyagbemi AA, Omobowale TO, Ola-Davies OE, Asenuga ER, Ajibade TO, Adejumobi OA, Afolabi JM, Ogunpolu BS, Falayi OO, Saba AB, *et al*: Luteolin-mediated Kim-1/NF-kB/Nrf2 signaling pathways protects sodium fluoride-induced hypertension and cardiovascular complications. Biofactors 44: 518-531, 2018.
29. Baiyun R, Li S, Liu B, Lu J, Lv Y, Xu J, Wu J, Li J, Lv Z and Zhang Z: Luteolin-mediated PI3K/AKT/Nrf2 signaling pathway ameliorates inorganic mercury-induced cardiac injury. Ecotoxicol Environ Saf 161: 655-661, 2018.
30. Parker MM, Shelhamer JH, Bacharach SL, Green MV, Natanson C, Frederick TM, Damske BA and Parrillo JE: Profound but reversible myocardial depression in patients with septic shock. Ann Intern Med 100: 483-490, 1984.
31. Sato R and Nasu M: A review of sepsis-induced cardiomyopathy. J Intensive Care 3: 48, 2015.
32. Sagy M, Al-Qaqaa Y and Kim P: Definitions and pathophysiology of sepsis. Curr Probl Pediatr Adolesc Health Care 43: 260-263, 2013.
33. Chousterman BG, Swirski FK and Weber GF: Cytokine storm and sepsis disease pathogenesis. Semin Immunopathol 39: 517-528, 2017.
34. Antonucci E, Fiaccadori E, Donadello K, Taccone FS, Franchi F and Scolletta S: Myocardial depression in sepsis: From pathogenesis to clinical manifestations and treatment. J Crit Care 29: 500-511, 2014.
35. Pathan N, Franklin JL, Eleftherohorinou H, Wright VJ, Hemingway CA, Waddell SJ, Griffiths M, Dennis JL, Relman DA, Harding SE and Levin M: Myocardial depressant effects of interleukin 6 in meningococcal sepsis are regulated by p38 mitogen-activated protein kinase. Crit Care Med 39: 1692-1711, 2011.
36. Vincent JL, Bakker J, Marecaux G, Schandene L, Kahn RJ and Dupont E: Administration of anti-TNF antibody improves left ventricular function in septic shock patients. Results of a pilot study. Chest 101: 810-815, 1992.

37. Brealey D and Singer M: Mitochondrial dysfunction in sepsis. Curr Infect Dis Rep 5: 365-371, 2003.
38. Unuma K, Aki T, Funakoshi T, Hashimoto K and Uemura K: Extrusion of mitochondrial contents from lipopolysaccharide-stimulated cells: Involvement of autophagy. Autophagy 11: 1520-1536, 2015.
39. Duran-Bedolla J, Montes de Oca-Sandoval MA, Saldana-Navor V, Villalobos-Silva JA, Rodriguez MC and Rivas-Arancibia S: Sepsis, mitochondrial failure and multiple organ dysfunction. Clin Invest Med Med 37: E58-E69, 2014.
40. Garrabou G, Moren C, Lopez S, Tobias E, Cardellach F, Miro O and Casademont J: The effects of sepsis on mitochondria. J Infect Dis 205: 392-400, 2012.
41. Neviere R, Fauvel H, Chopin C, Formstecher P and Marchetti P: Caspase inhibition prevents cardiac dysfunction and heart apoptosis in a rat model of sepsis. Am J Respir Crit Care Med 163: 218-225, 2001.
42. Terman A and Brunk UT: Autophagy in cardiac myocyte homeostasis, aging, and pathology. Cardiovasc Res 68: 355-365, 2005.
43. Gustafsson AB and Gottlieb RA: Eat your heart out: Role of autophagy in myocardial ischemia/reperfusion. Autophagy 4: 416-421, 2008.
44. Hsieh CH, Pai PY, Hsueh HW, Yuan SS and Hsieh YC: Complete induction of autophagy is essential for cardioprotection in sepsis. Ann Surg 253: 1190-1200, 2011.
45. Zhao X, Qi H, Zhou J, Xu S and Gao Y: P27 Protects cardiomyocytes from sepsis via activation of autophagy and inhibition of apoptosis. Med Sci Monit 24: 8565-8576, 2018.
46. Zhang BC, Zhang CW, Wang C, Pan DF, Xu TD and Li DY: Luteolin attenuates foam cell formation and apoptosis in Ox-LDL-stimulated macrophages by enhancing autophagy. Cell Physiol Biochem 39: 2065-2076, 2016.
47. Cao Z, Zhang H, Cai X, Fang W, Chai D, Wen Y, Chen H, Chu F and Zhang Y: Luteolin promotes cell apoptosis by inducing autophagy in hepatocellular carcinoma. Cell Physiol Biochem 43: 1803-1812, 2017.
48. Carling D: AMPK signalling in health and disease. Curr Opin Cell Biol 45: 31-37, 2017.
49. Garcia D and Shaw RJ: AMPK: Mechanisms of cellular energy sensing and restoration of metabolic balance. Mol Cell 66: 789-800, 2017.
50. Khan SH and Kumar R: Role of an intrinsically disordered conformation in AMPK-mediated phosphorylation of ULK1 and regulation of autophagy. Mol Biosyst 8: 91-96, 2012.
51. Kurumbail RG and Calabrese MF: Structure and regulation of AMPK. Exp Suppl 107: 3-22, 2016.
52. Ou HC, Pandey S, Hung MY, Huang SH, Hsu PT, Day CH, Pai P, Viswanadha VP, Kuo WW and Huang CY: Luteolin: A natural flavonoid enhances the survival of HUVECs against oxidative stress by modulating AMPK/PKC pathway. Am J Chin Med 47: 541-557, 2019.
53. Li J, Dong JZ, Ren YL, Zhu JJ, Cao JN, Zhang J and Pan LL: Luteolin decreases atherosclerosis in LDL receptor-deficient mice via a mechanism including decreasing AMPK-SIRT1 signaling in macrophages. Exp Ther Med 16: 2593-2599, 2018.
54. Zhang L, Han YJ, Zhang X, Wang X, Bao B, Qu W and Liu J: Luteolin reduces obesity-associated insulin resistance in mice by activating AMPKα1 signalling in adipose tissue macrophages. Diabetologia 59: 2219-2228, 2016.